

Supporting Information

Exceptionally Strong Electronic Coupling in Crystalline Perylene Diimides via Tuning

*Chenming Xue and Shi Jin**

Email: Shi.jin@csi.cuny.edu

Table of Contents

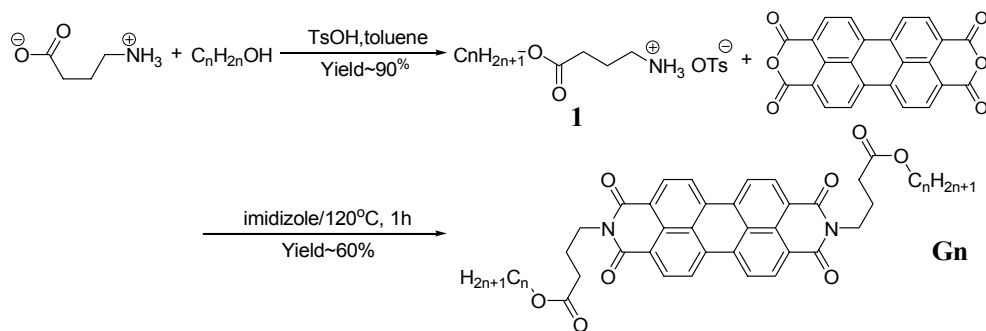
1. Materials	Page S3
2. Sample characterization.....	Page S3
3. Synthesis.....	Page S3
4. Figure S1.....	Page S13
5. Figure S2.....	Page S13
6. Figure S3.....	Page S14
7. Figure S4.....	Page S15
8. Figure S5.....	Page S17
9. Figure S6.....	Page S17
10. Figure S7.....	Page S18
11. Figure S8.....	Page S18
12. Figure S9.....	Page S19
13. Figure S10.....	Page S20
14. Figure S11.....	Page S20
15. Table S 1.....	Page S21
16. Conformation of <i>n</i> -alkyl chains at room temperature and in the high temperature phase.....	Page S22
17. Molecular simulation of PDI π -stacks in the high temperature phase.....	Page S22
18. References.....	Page S24

1. Materials. All reagents were used as received. 1-butanol (99+%), 1-hexanol (96%), 1-octanol (98%), 1-decanol (99%) and 1-dodecanol (98%) were purchased from Acros Organics. 1-tetradecanol (98+%) was purchased from TCI America. 1-Hexadecanol (98%) was purchased from Alfa Aesar. Toluene and acetone were purchased from Sigma-Aldrich. Imidazole was purchased from Fisher Scientific.

2. Sample characterization. ^1H NMR spectra were recorded on a Varian 300 MHz NMR spectrometer, with deuterated chloroform (CDCl_3) as solvent at 25 °C. The chemical shifts were reported using tetramethylsilane (TMS) as the internal standard. The NMR graphs and data were collected by using Spinworks 3 software. The peak at 7.26 ppm with two satellite peaks belongs to CHCl_3 residue in CDCl_3 . The peak at 1.58 ppm belongs to H_2O . Fourier transfer infrared spectra (FTIR) were recorded on a Bruker Vertex 70V spectrometer at the resolution of 1 cm^{-1} . A Thermo Electron 0019-200 heating cell (controlled by a Glas-Col DigiTrol II temperature controller) was used to heat specimen to collect FTIR spectra at high temperatures (HT). High resolution mass spectra (HRMS) were obtained at CUNY Mass Spectrometry Facility at Hunter College. UV-visible spectra were collected on a PerkinElmer Lambda UV-Vis spectrometer at the resolution of 1 nm. UV spectra shown in Figure 1b were collected from **Gn** in a 2/1 (v/v) methanol/chloroform binary solvent. Methanol with a calculated volume was added to a corresponding **Gn** chloroform solution (concentration = $2.65 \times 10^{-5}\text{ mol L}^{-1}$) which was stirred vigorously for a few seconds thereafter. The UV absorption spectrum was recorded after the solution was left aged for 30 minutes. For SEM studies, **Gn** aggregates were allowed to grow under the identical condition for UV measurements. Then **Gn** suspensions were dropped onto a conducting self-adhesive copper tape. After thorough evaporation of solvents, the specimen were coated with gold/palladium alloy in a BAL-TEC MED-020 coating system and imaged using an AMRAY 19101 scanning electron microscope. Solid **Gn** films for UV measurements were drop-cast from 2 mg mL^{-1} chloroform solutions and dried slowly in a jar saturated with chloroform vapor. A Mettler Toledo FP82HT hotstage (controlled by a Mettler Toledo FP90 central processor) was employed when collecting UV spectra at high temperatures. All peak positions were read from the second derivatives of the curves. X-ray diffraction measurements were performed on a Bruker Nanostar instrument with a $\text{Cu K}\alpha$ source and an image plate as the detector. A MRI heating stage was employed when collecting diffraction patterns at high temperatures. Solid samples for X-ray examination as in Figure S3 were precipitated from hot chloroform solutions when they cooled. DSC experiments were performed on a Perkin-Elmer PYRIS Diamond differential scanning calorimeter. Transition temperatures were determined using the onset temperatures and were calibrated using standard material (indium).

3. Synthesis:

General synthesis procedure for **Gn** is outlined below:



$n = 4, 6, 8, 10, 12, 14, 16$. TsOH: *p*-toluenesulfonic acid

General procedure of **1**

Into a 100 ml Schlenk flask were charged corresponding alcohol (35 mmol), 2.06 g (20 mmol) 4-aminobutyric acid, 4.2 g (22 mmol) p-toluenesulfonic acid monohydrate and 50 ml toluene. The mixture was purged with N₂ when it was heated to reflux (about 110 °C) for 8 hours. Subsequently the toluene was removed on a rotoevaporator and the remaining solid was dissolved in 80 ml acetone at 50 °C. The solution was then put in a refrigerator for crystallization. Subsequently, the crystalline solid was collected on a Buchner funnel by suction filtration and rinsed by 5 ml cold acetone. The recrystallization process was repeated for another time. The final white solid was dried in vacuum oven at room temperature (RT) until constant weight.

4-(butyloxy)-4-oxobutyl-1-ammonium 4-toluenesulfonate (**1a**)

The corresponding alcohol was 1-butanol, **n** = 4, yield **1a** 5.49g (83%)

4-(hexyloxy)-4-oxobutyl-1-ammonium 4-toluenesulfonate (**1b**)

The corresponding alcohol was 1-hexanol, **n** = 6, yield **1b** 6.39g (89%)

4-(octyloxy)-4-oxobutyl-1-ammonium 4-toluenesulfonate (**1c**)

The corresponding alcohol was 1-octanol, **n** = 8, yield **1c** 6.97g (90%)

4-(decyloxy)-4-oxobutyl-1-ammonium 4-toluenesulfonate (**1d**)

The corresponding alcohol was 1-decanol, **n** = 10, yield **1d** 7.64g (92%)

4-(dodecyloxy)-4-oxobutyl-1-ammonium 4-toluenesulfonate (**1e**)

The corresponding alcohol was 1-dodecanol, **n** = 12, yield **1e** 8.06g (91%)

4-(tetradecyloxy)-4-oxobutyl-1-ammonium 4-toluenesulfonate (**1f**)

The corresponding alcohol was 1-tetradecanol, **n** = 14, yield **1f** 8.67g (92%)

4-(hexadecyloxy)-4-oxobutyl-1-ammonium 4-toluenesulfonate (**1g**)

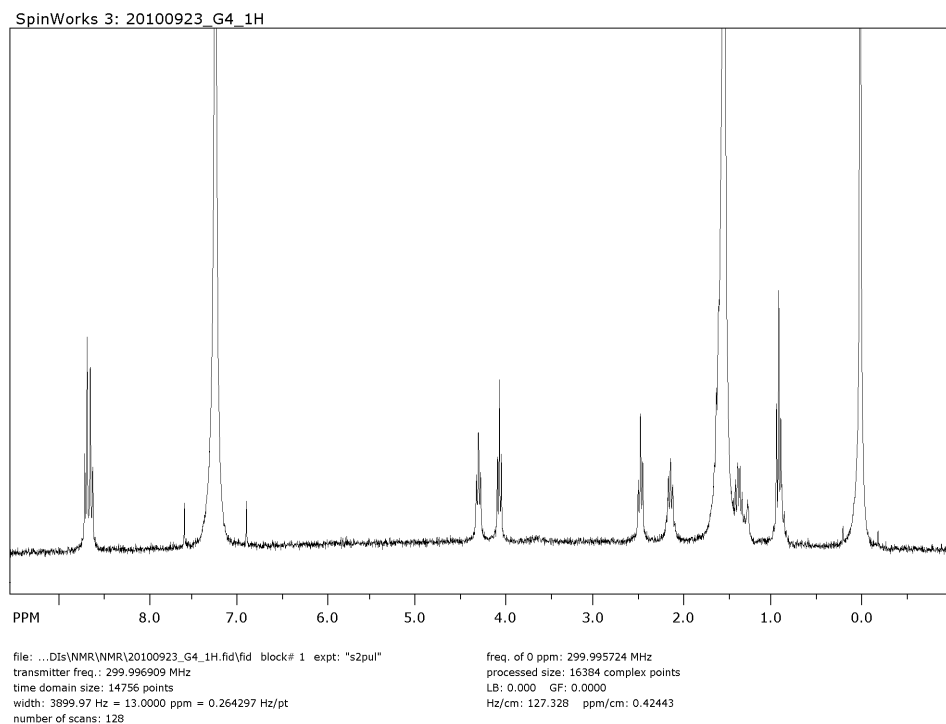
The corresponding alcohol was 1-hexadecanol, **n** = 16, yield **1g** 9.08g (91%)

General procedure of **Gn**

Into a 25 ml Schlenk flask were charged corresponding **1** (2 mmol), 392 mg (1 mmol) 3,4:9,10-perylenetetracarboxyldianhydride (PDA) and 4 g imidazole. The mixture was purged with N₂ for 15 minutes before being heated at 120 °C for one hour with stirring. Subsequently the reaction mixture was cooled to 90 °C. 15 ml deionized water was then added with the protection of N₂. The suspension was transferred to a 200 ml beaker and more deionized water was used to rinse the flask, to thoroughly transfer the solid. After suction filtration, the solid dispersion was repeatedly washed with 3% K₂CO₃ aqueous solution until the solution became colorless under a UV light (no yellow-green emission). The solid product was collected by suction-filtration and dried in a vacuum oven overnight at 60 °C. Then the dried solid was dissolved in 200 ml hot CHCl₃ (60 °C) and the insoluble residue was

removed by hot suction filtration. This process was performed again to further remove the insoluble particles at 60 °C. Afterwards, the solution was cooled down and left at RT for overnight to complete the crystallization. The solid was collected by suction filtration and rinsed with RT CHCl₃. This recrystallization process was applied again over night. The final solid was collected and dried in a vacuum oven at 40 °C overnight. For further purification, a hot chloroform solution (60 °C) with a concentration of about 5 mg ml⁻¹ was made and passed through a warm short silica gel column (3 cm long) quickly. A 10% methanol/CHCl₃ hot solution (60 °C) was used as the eluent. ¹H NMR, FTIR and HRMS confirmed the structure and purity of the compounds.

N,N'-di(4-(butyloxy)-4-oxobutyl)-3,4:9,10-perylenetetracarboxyldiimide (**G4**) Yield 0.371 g (55%)

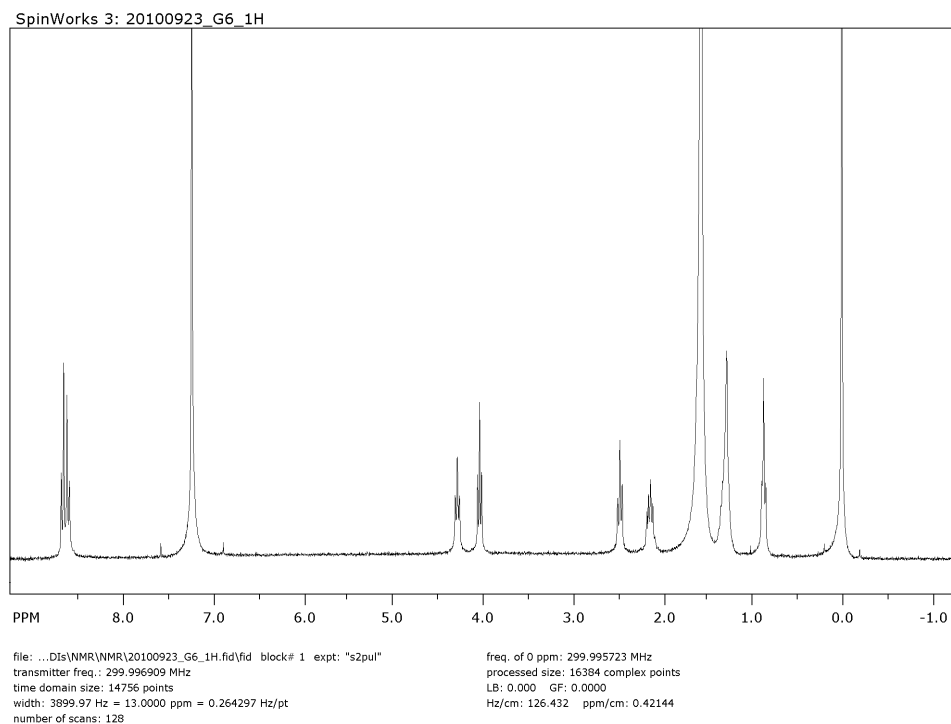


$^1\text{H NMR}$ (CDCl_3 , 300 MHz): δ (ppm) = 8.72 (d, J = 7.92 Hz, 4H, Ar), 8.65 (d, J = 7.78 Hz, 4H, Ar), 4.30 (t, J = 7.11 Hz, 4H, $\text{CH}_2\text{COOCH}_2$), 4.06 (t, J = 6.61 Hz, 4H, $\text{NCH}_2\text{CH}_2\text{CH}_2\text{COOCH}_2$), 2.48 (t, J = 7.68 Hz, 4H, $\text{NCH}_2\text{CH}_2\text{CH}_2\text{COOCH}_2$), 2.08 – 2.18 (m, 4H, $\text{NCH}_2\text{CH}_2\text{CH}_2\text{COOCH}_2$), 1.26 – 1.40 (m, $\text{CH}_2\text{COOCH}_2\text{CH}_2\text{CH}_2$), 0.92 (t, J = 7.23 Hz, 6H, $\text{COOCH}_2\text{CH}_2\text{CH}_2\text{CH}_3$). The resonance signal of $\text{CH}_2\text{COOCH}_2\text{CH}_2\text{CH}_2\text{CH}_3$ at about δ = 1.6 ppm is masked by the signal of water so that the exact position and area integration could not be obtained. Similarly, the multiplet of $\text{CH}_2\text{COOCH}_2\text{CH}_2\text{CH}_2\text{CH}_3$ (with maximum signal at δ = 1.38 ppm) is also under the strong influence of water signal so that the area integration could not be reliably performed.

FTIR (cm^{-1}): 2956 (antisymmetric CH_3), 2871 (symmetric CH_3), 1738 (ester $\text{C}=\text{O}$), 1691 (symmetric imide $\text{C}=\text{O}$ symmetric), 1660 (antisymmetric imide $\text{C}=\text{O}$), 1593 (aromatic ring stretch).

HRMS ($\text{M}+\text{H}$) $^+$: calcd for $\text{C}_{40}\text{H}_{39}\text{N}_2\text{O}_8^+$ 675.2701; found 675.2694.

N,N'-di(4-(hexyloxy)-4-oxobutyl)-3,4:9,10-perylenetetracarboxyldiimide (**G6**) Yield 0.438 g (60%)

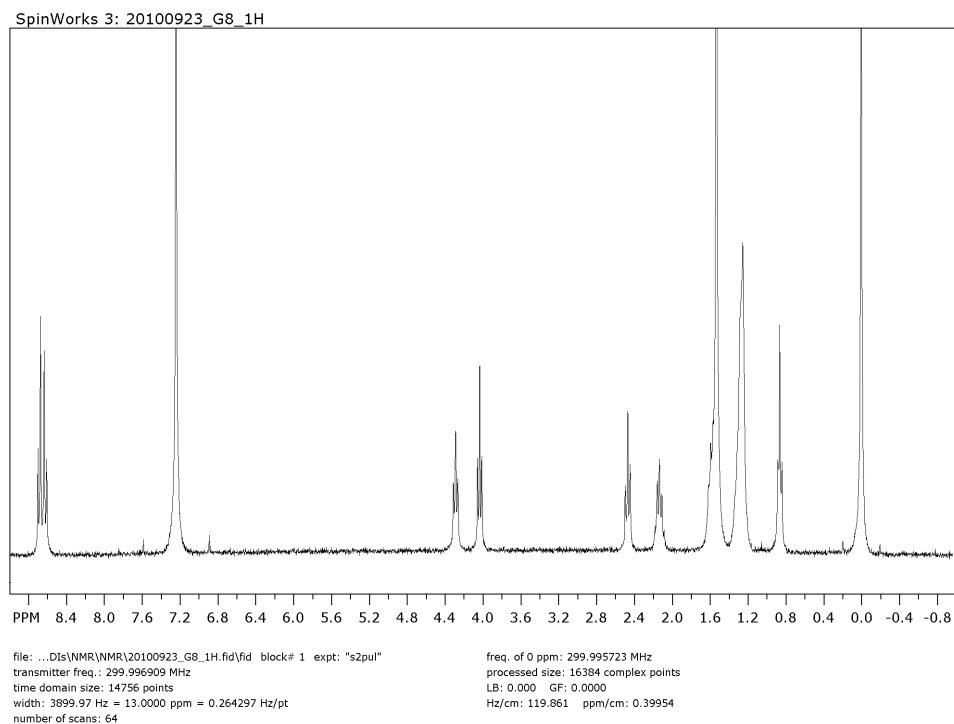


$^1\text{H NMR}$ (CDCl_3 , 300 MHz): δ (ppm) = 8.70 (d, J = 8.08 Hz, 4H, Ar), 8.64 (d, J = 7.93 Hz, 4H, Ar), 4.29 (t, J = 7.25 Hz, 4H, $\text{CH}_2\text{COOCH}_2$), 4.04 (t, J = 6.81 Hz, 4H, $\text{NCH}_2\text{CH}_2\text{CH}_2\text{COOCH}_2$), 2.48 (t, J = 7.43 Hz, 4H, $\text{NCH}_2\text{CH}_2\text{CH}_2\text{COOCH}_2$), 2.08 – 2.17 (m, 4H, $\text{NCH}_2\text{CH}_2\text{CH}_2\text{COOCH}_2$), 1.28 – 1.37 (m, 12H, $\text{CH}_2\text{COOCH}_2\text{CH}_2\text{CH}_2\text{CH}_2\text{CH}_2$), 0.87 (t, J = 6.99 Hz, 6H, $\text{CH}_2\text{COOCH}_2\text{CH}_2\text{CH}_2\text{CH}_2\text{CH}_2\text{CH}_3$). The resonance signal of $\text{CH}_2\text{COOCH}_2\text{CH}_2\text{CH}_2$ at about δ = 1.6 ppm is masked by the signal of water so that the exact position and area integration could not be obtained.

FTIR (cm^{-1}): 2951 (antisymmetric CH_3), 2869 (symmetric CH_3), 1739 (ester $\text{C}=\text{O}$), 1690 (symmetric imide $\text{C}=\text{O}$ symmetric), 1661 (antisymmetric imide $\text{C}=\text{O}$), 1592 (aromatic ring stretch).

HRMS ($\text{M}+\text{H}$) $^+$: calcd for $\text{C}_{44}\text{H}_{47}\text{N}_2\text{O}_8$ 731.3327; found 731.3327.

N,N'-di(4-(octyloxy)-4-oxobutyl)-3,4:9,10-perylene-tetracarboxyldiimide (**G8**) Yield 0.488 g (62%)

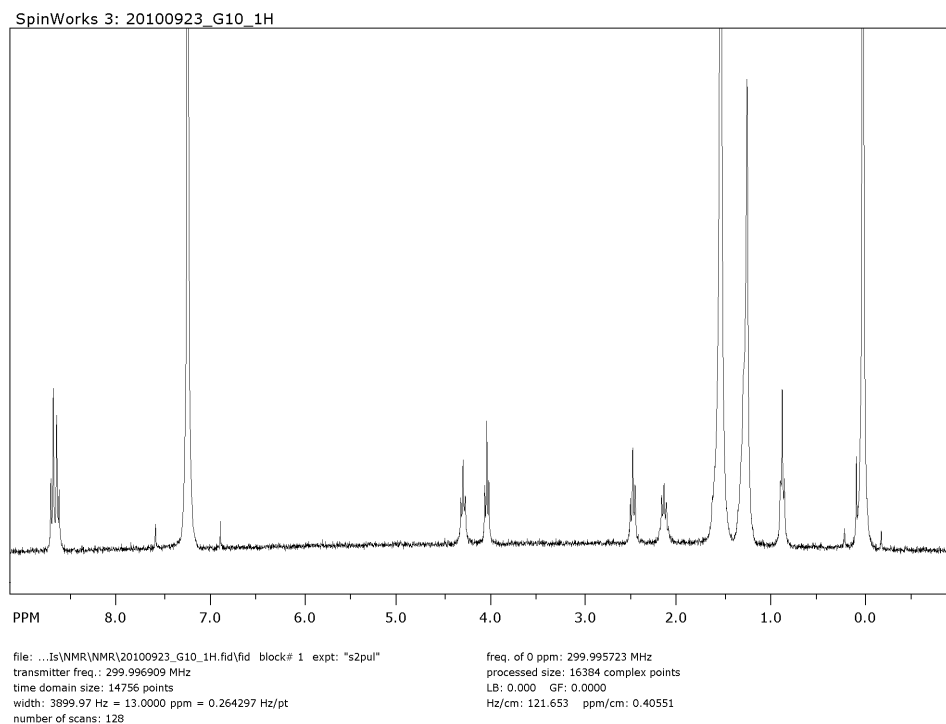


$^1\text{H NMR}$ (CDCl_3 , 300 MHz): δ (ppm) = 8.71 (d, J = 8.03 Hz, 4H, Ar), 8.66 (d, J = 8.08 Hz, 4H, Ar), 4.30 (t, J = 7.20 Hz, 4H, $\text{CH}_2\text{COOCH}_2$), 4.04 (t, J = 6.82 Hz, 4H, $\text{NCH}_2\text{CH}_2\text{CH}_2\text{COOCH}_2$), 2.48 (t, J = 7.55 Hz, 4H, $\text{NCH}_2\text{CH}_2\text{CH}_2\text{COOCH}_2$), 2.11 – 2.16 (m, 4H, $\text{NCH}_2\text{CH}_2\text{CH}_2\text{COOCH}_2$), 1.25 – 1.31 (m, 20H, $\text{CH}_2\text{COOCH}_2\text{CH}_2\text{CH}_2\text{CH}_2\text{CH}_2\text{CH}_2\text{CH}_2\text{CH}_2$), 0.86 (t, J = 6.55 Hz, 6H, $\text{CH}_2\text{COOCH}_2\text{CH}_2\text{CH}_2\text{CH}_2\text{CH}_2\text{CH}_2\text{CH}_2\text{CH}_3$). The resonance signal of $\text{CH}_2\text{COOCH}_2\text{CH}_2\text{CH}_2$ at about δ = 1.6 ppm is masked by the signal of water so that the exact position and area integration could not be obtained.

FTIR (cm^{-1}): 2927 (antisymmetric CH_2), 2850 (symmetric CH_2), 1743 (ester $\text{C}=\text{O}$), 1692 (symmetric imide $\text{C}=\text{O}$ symmetric), 1659 (antisymmetric imide $\text{C}=\text{O}$), 1592 (aromatic ring stretch).

HRMS ($\text{M}+\text{H}$) $^+$: calcd for $\text{C}_{48}\text{H}_{55}\text{N}_2\text{O}_8^+$ 787.3953; found 787.3948.

N,N'-di(4-(decyloxy)-4-oxobutyl)-3,4,9,10-perylenetetracarboxyldiimide (**G10**) Yield 0.556 g (66%)

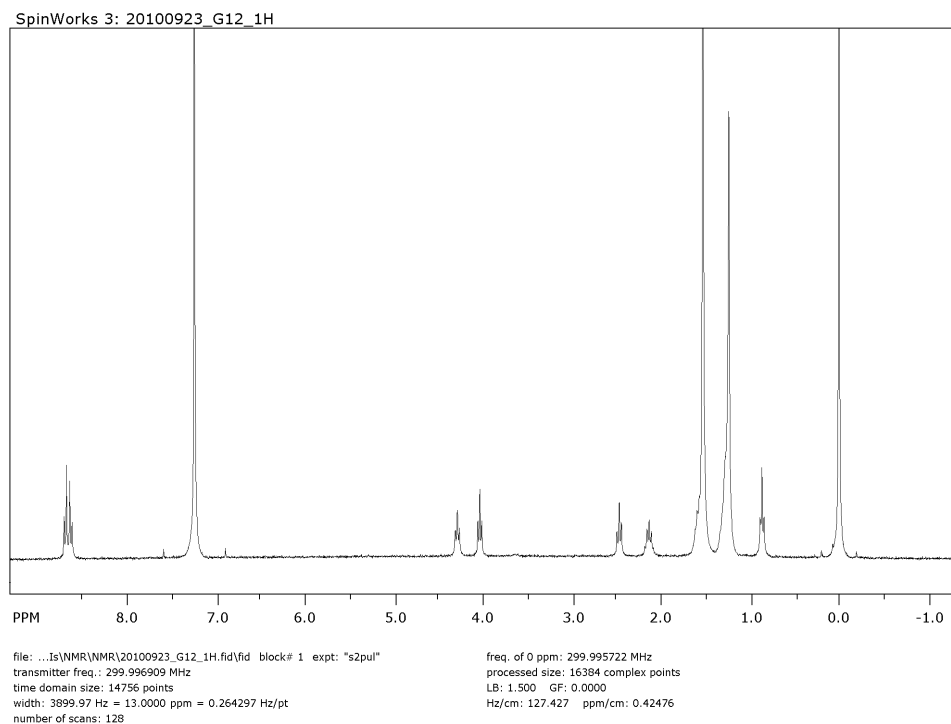


$^1\text{H NMR}$ (CDCl_3 , 300 MHz): δ (ppm) = 8.72 (d, J = 8.02 Hz, 4H, Ar), 8.67 (d, J = 8.22 Hz, 4H, Ar), 4.30 (t, J = 6.94 Hz, 4H, $\text{CH}_2\text{COOCH}_2$), 4.04 (t, J = 6.69 Hz, 4H, $\text{NCH}_2\text{CH}_2\text{CH}_2\text{COOCH}_2$), 2.47 (t, J = 7.74 Hz, 4H, $\text{NCH}_2\text{CH}_2\text{CH}_2\text{COOCH}_2$), 2.09 – 2.19 (m, 4H, $\text{NCH}_2\text{CH}_2\text{CH}_2\text{COOCH}_2$), 1.24 – 1.29 (m, 28H, $\text{CH}_2\text{COOCH}_2\text{CH}_2\text{CH}_2\text{CH}_2\text{CH}_2\text{CH}_2\text{CH}_2\text{CH}_2\text{CH}_2$), 0.87 (t, J = 6.92 Hz, 6H, $\text{CH}_2\text{COOCH}_2\text{CH}_2\text{CH}_2\text{CH}_2\text{CH}_2\text{CH}_2\text{CH}_2\text{CH}_2\text{CH}_2\text{CH}_3$). The resonance signal of $\text{CH}_2\text{COOCH}_2\text{CH}_2\text{CH}_2$ at about δ = 1.6 ppm is masked by the signal of water so that the exact position and area integration could not be obtained.

FTIR (cm^{-1}): 2917 (antisymmetric CH_2), 2852 (symmetric CH_2), 1743 (ester $\text{C}=\text{O}$), 1692 (symmetric imide $\text{C}=\text{O}$ symmetric), 1658 (antisymmetric imide $\text{C}=\text{O}$), 1592 (aromatic ring stretch).

HRMS ($\text{M}+\text{H}$) $^+$: calcd for $\text{C}_{52}\text{H}_{63}\text{N}_2\text{O}_8^+$ 843.4579; found 843.4580.

N,N'-di(4-(dodecyloxy)-4-oxobutyl)-3,4:9,10-perylenetetracarboxyldiimide (**G12**) Yield 0.548 g (61%)

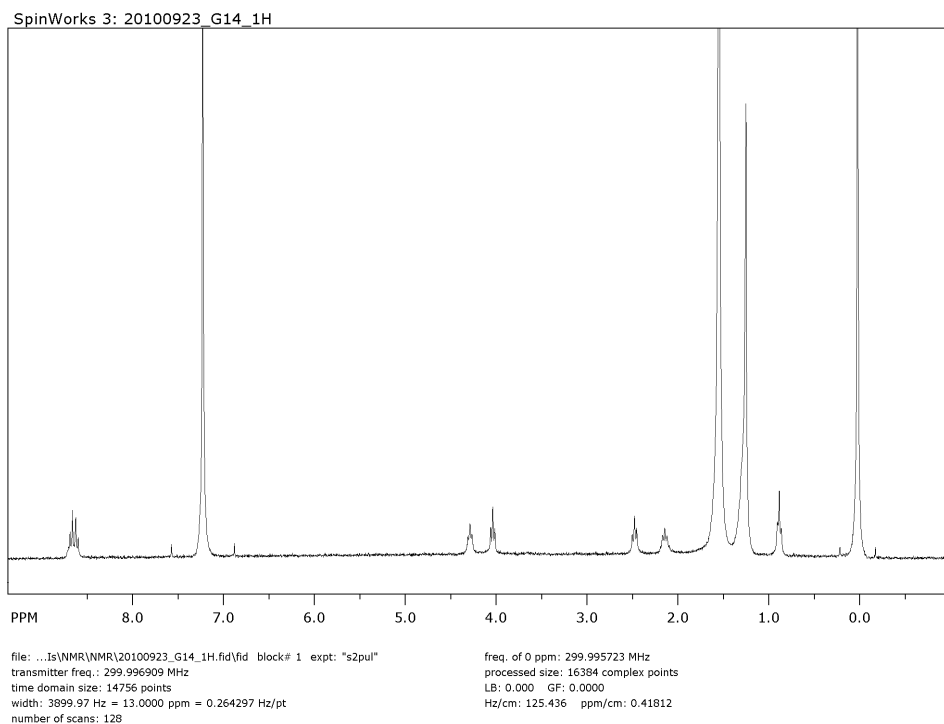


$^1\text{H NMR}$ (CDCl_3 , 300 MHz): δ (ppm) = 8.71 (d, J = 7.90 Hz, 4H, Ar), 8.65 (d, J = 8.20 Hz, 4H, Ar), 4.30 (t, J = 7.20 Hz, 4H, $\text{CH}_2\text{COOCH}_2$), 4.04 (t, J = 6.61 Hz, 4H, $\text{NCH}_2\text{CH}_2\text{CH}_2\text{COOCH}_2$), 2.47 (t, J = 7.65 Hz, 4H, $\text{NCH}_2\text{CH}_2\text{CH}_2\text{COOCH}_2$), 2.09 – 2.18 (m, 4H, $\text{NCH}_2\text{CH}_2\text{CH}_2\text{COOCH}_2$), 1.24 – 1.29 (m, 36H, $\text{CH}_2\text{COOCH}_2\text{CH}_2\text{CH}_2\text{CH}_2\text{CH}_2\text{CH}_2\text{CH}_2\text{CH}_2\text{CH}_2\text{CH}_2\text{CH}_2$), 0.87 (t, J = 6.34 Hz, 6H, $\text{CH}_2\text{COOCH}_2\text{CH}_2\text{CH}_2\text{CH}_2\text{CH}_2\text{CH}_2\text{CH}_2\text{CH}_2\text{CH}_2\text{CH}_2\text{CH}_2\text{CH}_3$). The resonance signal of $\text{CH}_2\text{COOCH}_2\text{CH}_2\text{CH}_2$ at about δ = 1.6 ppm is masked by the signal of water so that the exact position and area integration could not be obtained.

FTIR (cm^{-1}): 2916 (antisymmetric CH_2), 2852 (symmetric CH_2), 1744 (ester $\text{C}=\text{O}$), 1692 (symmetric imide $\text{C}=\text{O}$ symmetric), 1660 (antisymmetric imide $\text{C}=\text{O}$), 1593 (aromatic ring stretch).

HRMS ($\text{M}+\text{H}$) $^+$: calcd for $\text{C}_{56}\text{H}_{71}\text{N}_2\text{O}_8^+$ 899.5205; found 899.5199.

N,N'-di(4-(tetradecyloxy)-4-oxobutyl)-3,4:9,10-perylenetetracarboxyldiimide (**G14**) Yield 0.621 g (65%)



$^1\text{H NMR}$ (CDCl_3 , 300 MHz): δ (ppm) = 8.72 (d, J = 8.07 Hz, 4H, Ar), 8.66 (d, J = 7.74 Hz, 4H, Ar), 4.30 (t, J = 6.59 Hz, 4H, $\text{CH}_2\text{COOCH}_2$), 4.04 (t, J = 6.72 Hz, 4H, $\text{NCH}_2\text{CH}_2\text{CH}_2\text{COOCH}_2$), 2.47 (t, J = 7.17 Hz, 4H, $\text{NCH}_2\text{CH}_2\text{CH}_2\text{COOCH}_2$), 2.11 – 2.16 (m, 4H, $\text{NCH}_2\text{CH}_2\text{CH}_2\text{COOCH}_2$), 1.24 – 1.28 (m, 44H, $\text{CH}_2\text{COOCH}_2\text{CH}_2\text{CH}_2\text{CH}_2\text{CH}_2\text{CH}_2\text{CH}_2\text{CH}_2\text{CH}_2\text{CH}_2\text{CH}_2\text{CH}_2\text{CH}_2\text{CH}_2\text{CH}_2\text{CH}_2$), 0.87 (t, J = 6.26 Hz, 6H, $\text{CH}_2\text{COOCH}_2\text{CH}_2\text{CH}_2\text{CH}_2\text{CH}_2\text{CH}_2\text{CH}_2\text{CH}_2\text{CH}_2\text{CH}_2\text{CH}_2\text{CH}_2\text{CH}_2\text{CH}_2\text{CH}_3$). The resonance signal of $\text{CH}_2\text{COOCH}_2\text{CH}_2\text{CH}_2$ at about δ = 1.6 ppm is masked by the signal of water so that the exact position and area integration could not be obtained.

FTIR (cm^{-1}): 2916 (antisymmetric CH_2), 2852 (symmetric CH_2), 1746 (ester $\text{C}=\text{O}$), 1692 (symmetric imide $\text{C}=\text{O}$ symmetric), 1660 (antisymmetric imide $\text{C}=\text{O}$), 1593 (aromatic ring stretch).

HRMS ($\text{M}+\text{H}$) $^+$: calcd for $\text{C}_{60}\text{H}_{79}\text{N}_2\text{O}_8^+$ 955.5831; found 955.5823.

Figure S1. UV spectra of **Gn** dilute solutions. Absorbance values were normalized for an easy comparison.

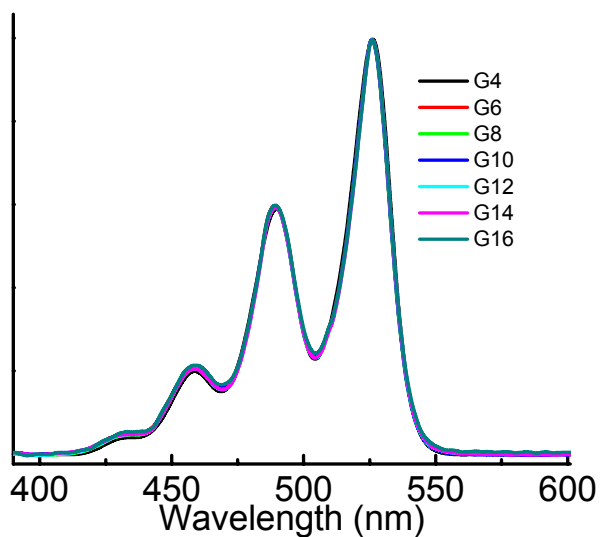


Figure S2. The UV absorption spectra of **Gn** solid films drop-cast from chloroform solutions. The absorbance values were normalized at the λ_{max} for an easy comparison.

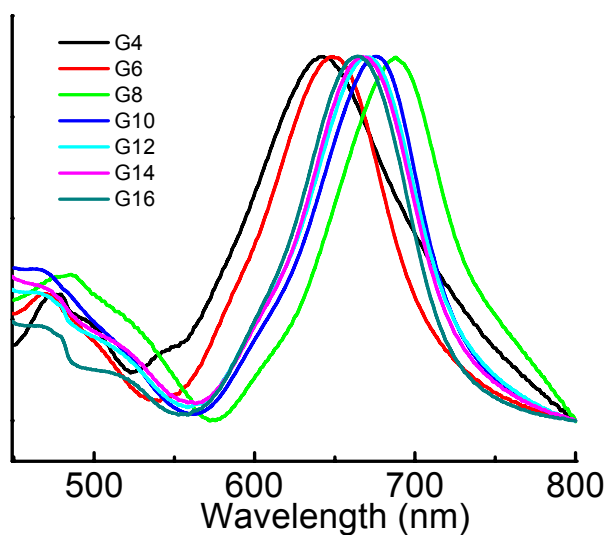


Figure S3. Wide angle X-ray diffraction patterns of solid **Gn**. Si: the diffraction from silicon powder which was added as the internal calibration standard.

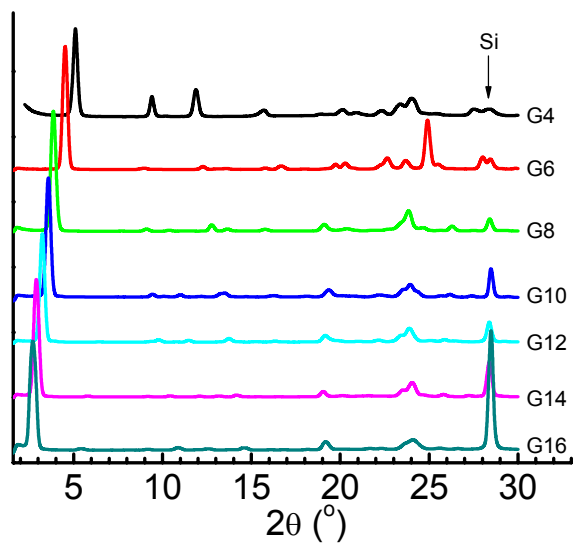
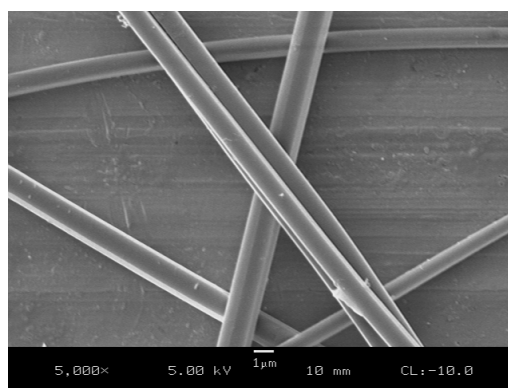
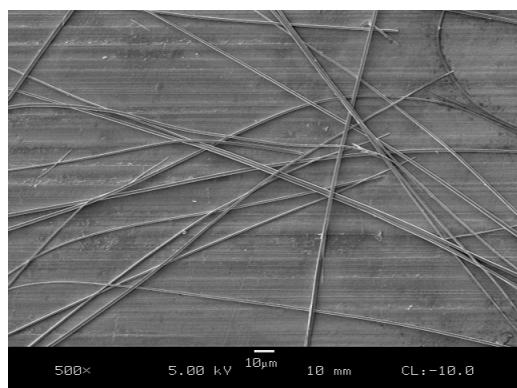
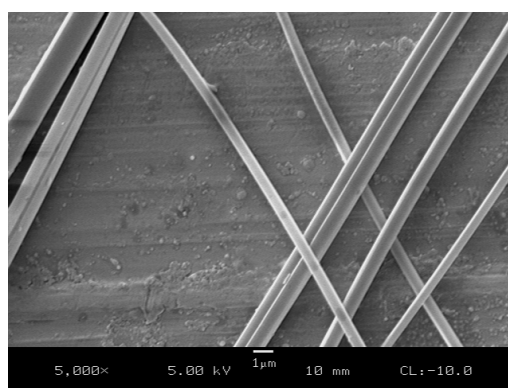
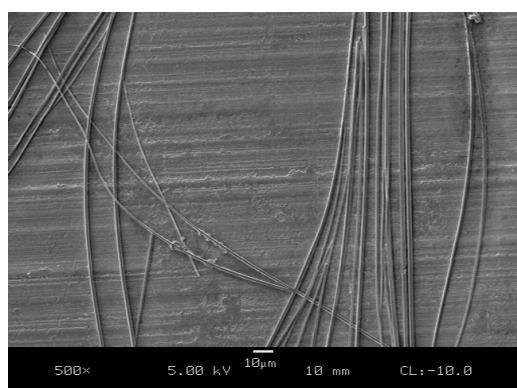


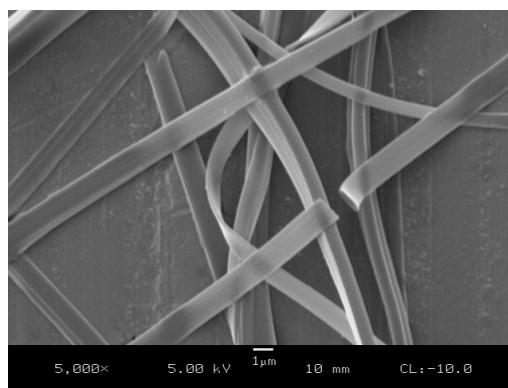
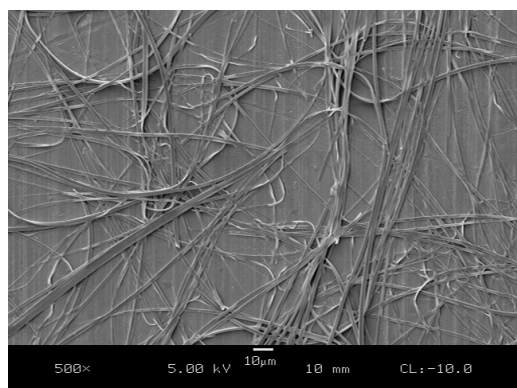
Figure S4. SEM images of **Gn** aggregates grown from 2/1 (v/v) methanol/chloroform binary solvent (left: lower magnification; right: higher magnification).



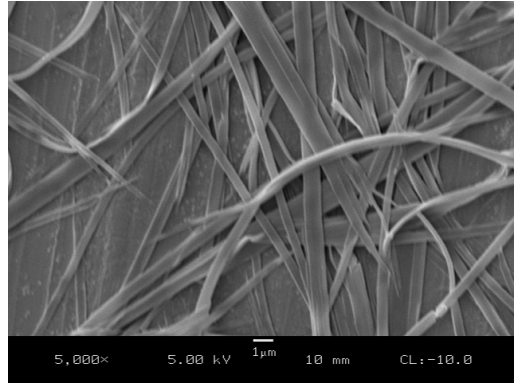
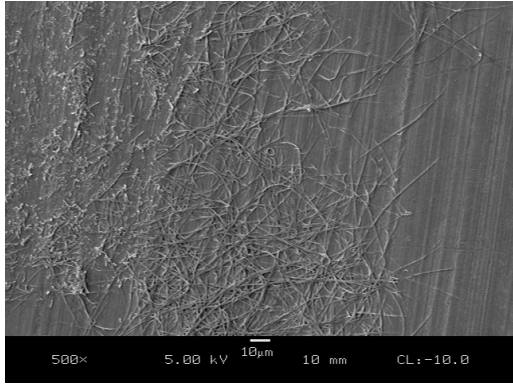
G4



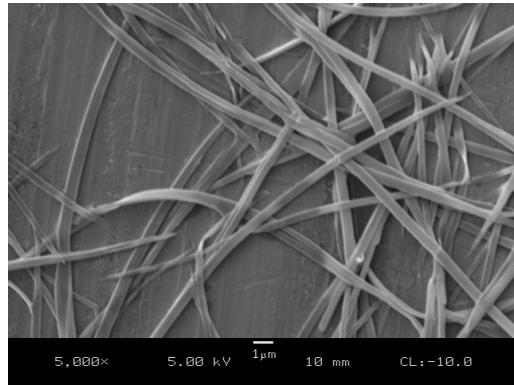
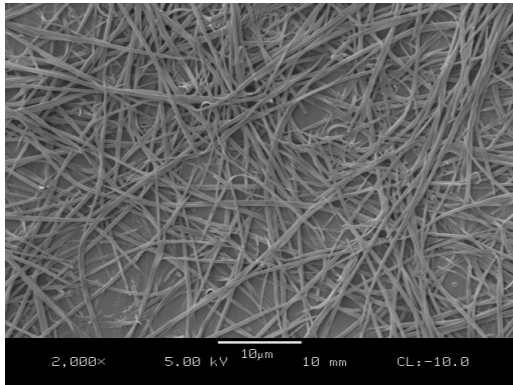
G6



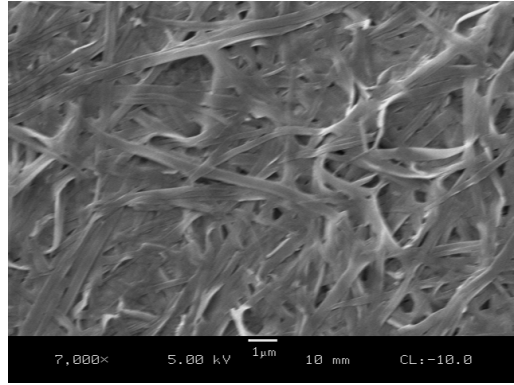
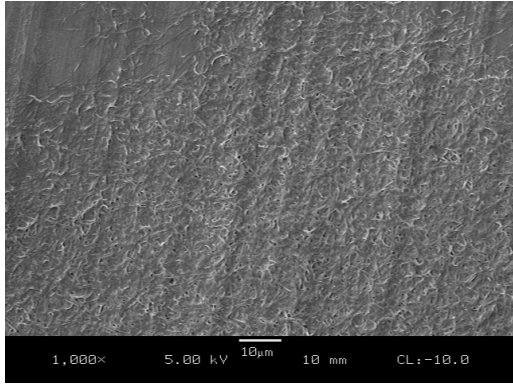
G8



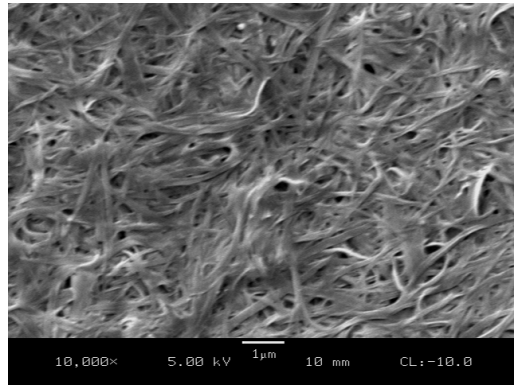
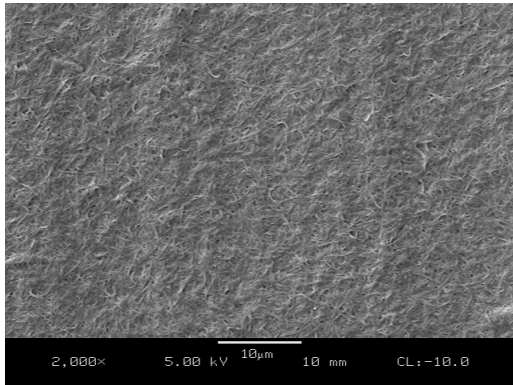
G10



G12



G14



G16

Figure S5. Ester $\nu_{C=O}$ region of **Gn** at room temperature

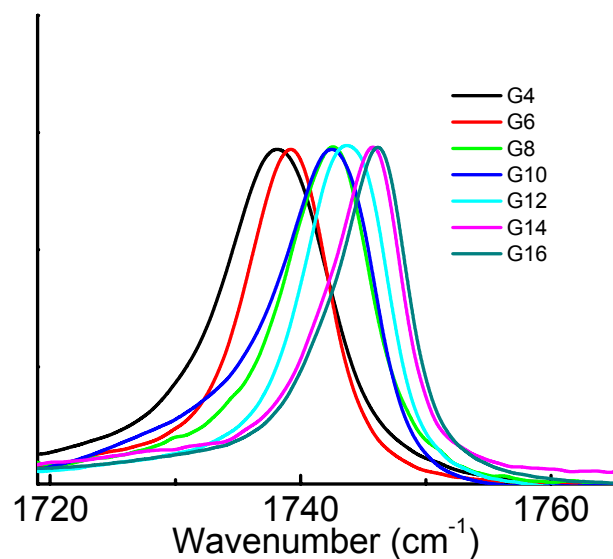


Figure S6. CH_2 stretching region of **Gn**: A) at room temperature; B) in the high temperature phase (spectra were taken at 160 °C for G8-G16, 170 °C for G6 and 180 °C for G4). Peak maximum frequency values were represented by dash lines.

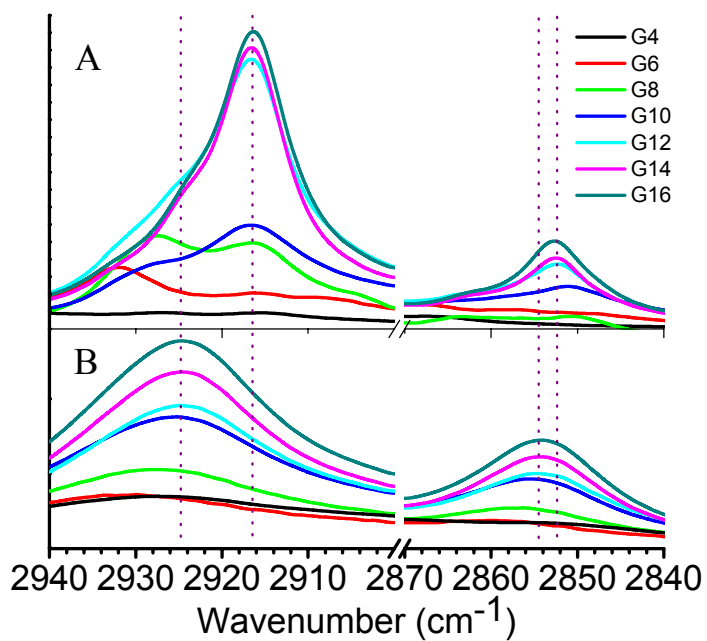


Figure S7. CH₂ scissoring region of **Gn**: A) at room temperature; B) in the high temperature phase (spectra were taken at 160 °C for **G8-G16**, 170 °C for **G6** and 180 °C for **G4**)

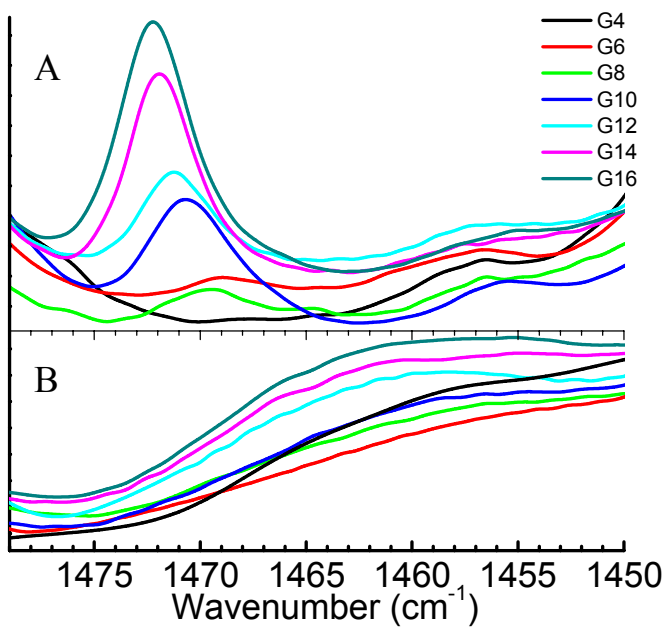


Figure S8. Ester $\nu_{C=O}$ region of **Gn** in the high temperature phase (spectra were taken at 160 °C for **G8-G16**, 170 °C for **G6** and 180 °C for **G4**)

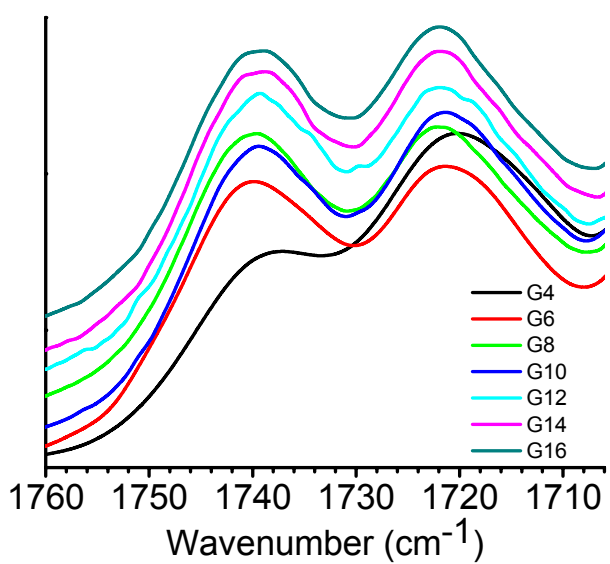


Figure S9. Wide angle X-ray diffraction patterns of solid **Gn** in the high temperature phase (spectra were taken at 160 °C for **G8-G16**, 170 °C for **G6** and 180 °C for **G4**). Si: the diffraction from silicon powder which was added as the internal calibration standard.

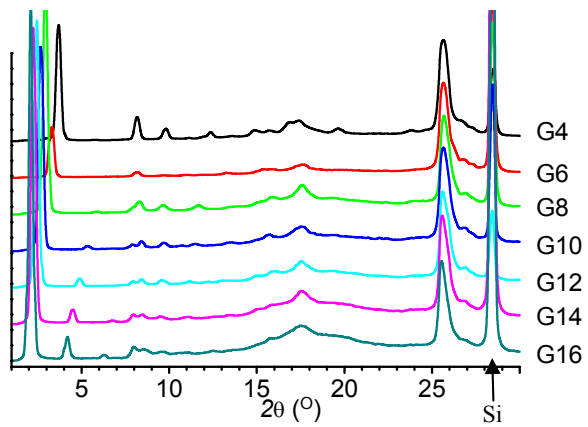


Figure S10. The conformation of single **G1** with the lowest energy (left: side view; right: tilt view)

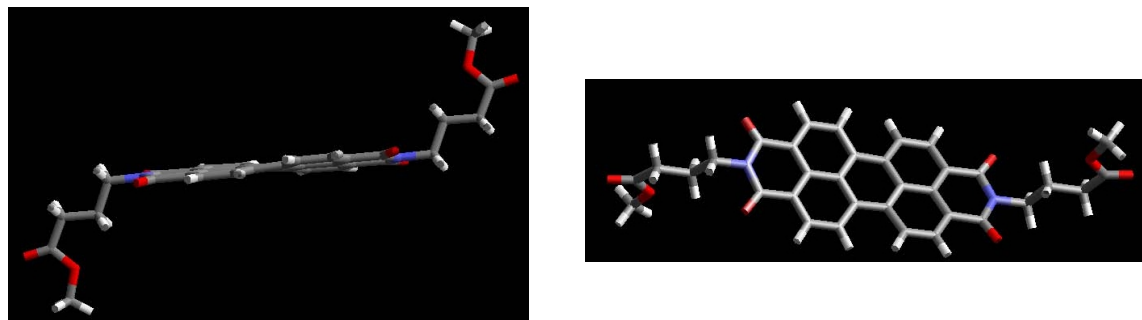


Figure S11. The 1D π -stacked **G1** crystal (the high temperature phase) with the lowest energy (left: top view; middle: side view; right: tilt view), one set of molecules were shadowed for the sake of clarity.

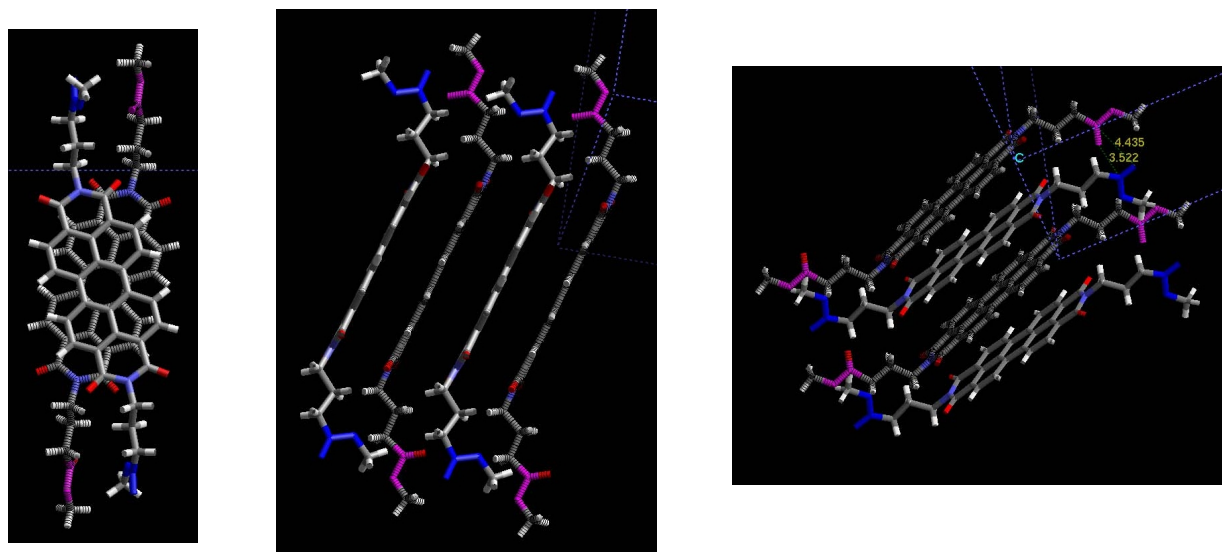


Table S1. C-H stretching vibration frequency values and transition temperatures of **G_n**

n	RT*		HT*		T₁ (°C)*	T₂ (°C)*
	v_{as}(CH₂) (cm⁻¹)	v_s(CH₂) (cm⁻¹)	v_{as}(CH₂) (cm⁻¹)	v_s(CH₂) (cm⁻¹)		
4					175.3	>350
6					164.8	348.7
8	2915.6	2850.5	2927.9	2856.1	147.6	344.9
10	2916.7	2851.1	2925.1	2855.5	137.8	337.4
12	2916.3	2852.2	2923.9	2854.6	131.6	325.9
14	2916.5	2852.4	2923.2	2854.2	128.3	319.4
16	2916.2	2852.7	2923.4	2854.2	122.6	311.7

RT: room temperature phase

HT: high temperature phase, spectra were taken at 160 °C for **G8-G16**, 170 °C for **G6** and 180 °C for **G4**

T₁: the transition temperature between the RT and HT

T₂: the isotropization temperature of HT

4. Conformation of *n*-alkyl chains at room temperature and in the high temperature phase

The phase transition behaviors of **Gn**s are summarized in Table S1. Between the room temperature crystalline phase and the isotropic liquid phase, every **Gn** also exhibits a high temperature phase. While the color of **Gn**s at room temperature is typically green, the color in the high temperature phase is red.

It is known that the frequencies of asymmetric stretching ($\nu_{\text{as}}(\text{CH}_2)$) and symmetric stretching ($\nu_{\text{s}}(\text{CH}_2)$) of *n*-alkyl chains are sensitive to their conformation. The $\nu_{\text{as}}(\text{CH}_2)$ and $\nu_{\text{s}}(\text{CH}_2)$ values for an all-anti alkyl chain are typically in the ranges of 2916 to 2920 and 2846 to 2850 cm^{-1} , respectively. These ranges shift to 2924–2928 and 2854–2856 cm^{-1} for liquid-like disordered chains.^[1] The CH_2 stretching region of **Gn** at room temperature is shown in Figure S6. For $n \geq 8$, the $\nu_{\text{as}}(\text{CH}_2)$ and $\nu_{\text{s}}(\text{CH}_2)$ bands are clearly visible at about 2916 and 2851 cm^{-1} respectively. The frequency values are listed in Table S1. The $\nu_{\text{as}}(\text{CH}_2)$ values point to planar all-anti *n*-alkyl chains, while the $\nu_{\text{s}}(\text{CH}_2)$ values suggest that *n*-alkyl chains may contain a small number of gauche bonds. Typically, for partially disordered *n*-alkyl chains such as those found in *n*-alkane rotator phases, the CH_2 scissoring band appears as a relative broad peak at 1466 cm^{-1} .^[2] As shown in Figure S7, the CH_2 scissoring band of **Gn** can be found at about 1471 cm^{-1} as a sharp peak, which strongly indicate that the dominant conformation of *n*-alkyl chains is all-anti.^[2a]

In contrast, in the high temperature phase, as shown in Table S1 and Figure S6, $\nu_{\text{as}}(\text{CH}_2)$ and $\nu_{\text{s}}(\text{CH}_2)$ of **Gn** peak at about 2924 and 2855 cm^{-1} , respectively. These values propose liquid-like disordered *n*-alkyl chains in this phase. The CH_2 scissoring region presented in Figure S7 shows only very broad bands, which supports the assignment of liquid-like *n*-alkyl chain conformation. Such disordered chains are expected to exhibit a broad diffraction with the peak maximum around 4.6 Å ($2\theta \approx 19.3^\circ$), and this is indeed the case as shown in Figure S9, especially when the **n** value is large. The PDI cores are clearly π -stacked in this high temperature phase as indicated by the strong diffraction peak at about 25.6° 2θ angle.

5. Molecular simulation of PDI π -stacks in the high temperature phase

The ester stretching region of the high temperature phase is shown in Figure S8. In sharp contrast with room temperature phase, every **Gn** exhibits two ester $\nu_{\text{C=O}}$ bands and the peak positions are independent of the length of *n*-alkyl chains.

To understand the origin of two ester $\nu_{\text{C=O}}$ bands, molecular modeling was carried out using a Cerius 2 software package (version 4.10) with the COMPASS force field. For clarity, methyl groups were employed as *n*-alkyl groups (**G1**). As the first step, the adjustable dihedral angles were systematically altered to find the lowest energy conformation of a single **G1**, which is shown in Figure S10. In the second step, Two **G1** molecules were placed in an unit cell with P1 symmetry and unit cell parameters α , β and γ were all set to 90° . The perylene ring planes are arranged approximately parallel to the *ab* plane. The lattice parameters, *a* and *b*, were set to 5 nm to avoid inter stack interactions. The initial inter-planar spacing between two perylene rings was set as 3 to 6 Å, and then energy of this 1D crystal was minimized. During energy minimization, the unit cell angles and *a*, *b* were fixed but *c* was unrestricted with an initial value of 1.2 nm. All the adjustable dihedral angles were systematically altered, as long as

the energy of the resulting single **G1** is no more than 3 kcal higher than the one with the lowest energy. The final 1D crystal structure with the lowest energy is shown in Figure S11. It is important to note that the energy-minimized structure is independent on the initial states of two molecules.

The inter-planar separation between two perylene rings is about 3.34 Å. The rotation angle between the long axes of two adjacent perylene rings is about 28.5°. It is interesting to see that in the energy-minimized structure, there are indeed two crystallographically nonequivalent types of ester groups (one in blue, one in pink). C=O bond lengths are 1.210 Å and 1.206 Å for the blue and pink ester groups, respectively. This can qualitatively explain the observation of two ester $\nu_{\text{C=O}}$ bands, as it is well known that longer C=O bond is weaker, which corresponds to a lower $\nu_{\text{C=O}}$ frequency. The simulation result also supports the presence of ester dipole-dipole interaction. As shown in Figure S11 (right), the shortest distance between the oxygen atom of a blue ester group to the carbonyl carbon of a pink ester group is 4.435 Å. The shortest distance between the oxygen atom of a pink ester group to the carbonyl carbon of a blue ester group is only 3.522 Å. Such short distances imply that ester groups are engaged in appreciable dipole-dipole attractive interaction. Especially the distance of 3.522 Å points to a strong dipole-dipole interaction.

References

- [1]. a) R. G. Snyder, H. L. Strauss, C. A. Elliger, *J. Phys. Chem.* **1982**, *86*, 5145. b) N. V. Venkataraman, S. Vasudevan, *J. Phys. Chem. B* **2001**, *105*, 1805.
- [2]. a) K. Sasaki, N. Inayoshi, K. Tashiro, *J. Phys. Chem. C* **2009**, *113*, 3287. b) H. L. Casal, D. G. Cameron, H. M. Mantsch, *Can. J. Chem.* **1983**, *61*, 1736.